Long-Short Term Memory Based TALOS Wave Energy Converter Power Output Prediction with Numerical Modelling

*Yueqi Wu, Wanan Sheng, James Taylor, George Aggidis, Xiandong Ma**
School of Engineering, Lancaster University.
Lancaster, United Kingdom

ABSTRACT

Wave energy shows potential to provide electricity in a renewable manner. The TALOS WEC (Wave Energy Converter) is a unique design with six PTO (Power Take-Off) elements to provide six Degrees of Freedom (DOFs), which is potentially able to harvest energy more efficiently than traditional single-DOF devices. As a step towards its optimisation and control, a power prediction model is developed, using the wave elevation and motions of the WEC to predict the power output of each PTO. The results show that using LSTM (Long-Short Term Memory) has a higher prediction accuracy than the other approaches considered.

KEY WORDS: TALOS; WEC; power prediction; machine learning; LSTM

INTRODUCTION

Much research has been done on energy harvesting technologies over the past few decades, in part due to the incoming energy crisis. As a type of renewable energy, ocean waves provide significant energy via a sustainable and reliable approach. As a result, many different types of WECs have been designed and tested to produce clean and renewable energy (Li et al., 2012). Examples include Lancaster University's PS Frog (Taylor et al., 2002; McCabe et al., 2006), AquaBuOy (AquaBuOy, 2016), and Powerbuoy (Powerbuoy, 2016).

In general, WECs can be categorised as point absorbers, oscillating water columns, terminators, oscillating wave surge converters, attenuators, and submersed pressure differential devices (Aggidis and Taylor, 2017; Darwish and Aggidis, 2022). The majority of WECs are single-DOF devices, which means they could only extract energy from one direction of motion. Based on the single-DOF method, prototypes have been designed such as the Carnegie Wave Energy Limited prototypes (Wave Hub, 2016), the Archimedes Wave Swing (AWS Ocean, 2016), Oregon Limited's multi-resonant chamber (Orecon, 2009), and Salter's Duck (Salter, 1974). However, the kinetic power contained in the waves is in multiple directions. In hydrodynamic analysis, the waves have yaw, roll, and pitch motions in heave, surge, and sway axes, respectively. In total, there are six degrees of freedom in WECs that would be affected by the waves. Theoretically, if the device can extract energy from multiple DOFs, more energy can be thus generated.

Despite of the majority designs being single-DOF, few multi-DOF WECs have been developed to date. One of the most famous designs is Pelamis, which is a snake shape device with several tubes that are connected by hydraulic rams. The electricity is generated from the hydraulic rams that connect the moving tubes. Pelamis prototypes have been deployed in Portugal and Scotland and fed electricity in national grids (Boyle and Duckers, 2012).

Compared with single-DOF devices, multi-DOF WECs have seen much less research and prototype design. Development of Pelamis, for example, was cancelled because the company went into administration after being unable to secure the level of additional funding required for the further development of their technology (Wave power firm Pelamis calls in administrators, 2014). NHP-WEC (Novel High-performance Wave Energy Converter) is an ongoing project that aims to design a novel multi-DOF point absorber style WEC, called TALOS, built as a 1/100th scale representation, with a solid outer hull containing all the moving parts. These include a ball mass and dampers (PTOs) that connect the ball and the hull as shown in Fig. 1.

During the development of the prototype, ocean uncertainties threaten the reliability and stability of the ocean energy system, especially for WECs (Sanchez et al., 2018). Hence, it is necessary to forecast ocean wave energy to save construction and pilot project costs (Reikard et al., 2015). Prediction of WEC power output can bring the following benefits:

- Improve the design of the control system.

- Improve power management abilities.
- Improve the reliability of the condition monitoring system.

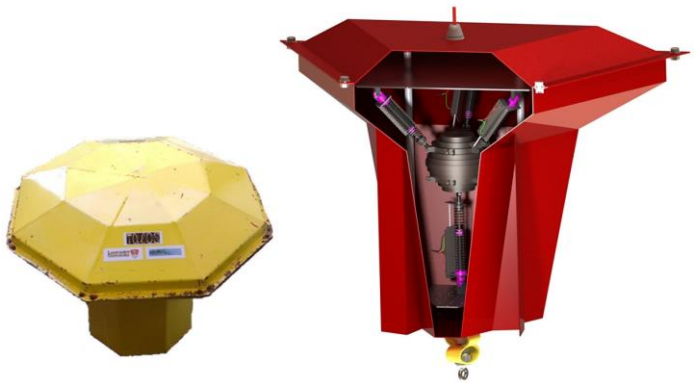

Fig. 1 TALOS I photograph (left) and TALOS II prototype diagram, with cut away section to show the internal PTO components (from Bhatt et al., 2016).

In existing research into ocean energy, most of the studies are focused on a wave prediction perspective. Desouky and Abdelkhalik (2019), for example, propose a method based on ANN (Artificial Neural Network) and NARX (nonlinear autoregressive network with exogenous inputs) to predict wave surface elevation. By contrast, considering the non-linearity of ocean waves, a variational Bayesian machine learning method is proposed to predict the wave elevation, uncertainty, and the predictable zone (Zhang et al., 2022). The latter results show that the prediction errors are 5.4% and 11.7% lower than linear wave theory and deterministic machine learning approaches, respectively.

However, predicting the power generation of a WEC is more complicated compared with wave prediction and can be a challenge since calculations involving the boundary condition equations are complex and time-consuming. Hence, researchers are seeking approaches to replace the numerical solutions (Mousavi et al., 2021). With the development of AI (Artificial Intelligence) and ML (Machine Learning) technologies, using ML to predict wave power has now became a reality (Bento et al., 2021). Genetic algorithms are adapted to produce prediction models by using different wave periods, wave heights, and water depths in simulation (Liu et al., 2020). Other methods, such as reinforcement learning, K-means clustering, and CNN (Convolutional Neural Network) are also employed to predict the electricity power generated from the WEC (Zou et al., 2022; Wang, 2020; and Ni et al., 2018).

In this context, the present paper proposes an LSTM based power prediction model for the multi-DOF TALOS device. The prediction results are compared with regression trees, SVR (Support Vector Regression) and ANN methods.

TALOS WEC POWER GENERATION PREDICTION MODEL

TALOS WEC model

Fig. 2 demonstrates the PTO structure of TALOS. The PTO system is composed of a heavy ball at the centre. Six dampers (PTOs) are used to connect the outside hull and the ball inside. Due to the weight of the ball, the ball would have relative motions to the hull when the incoming wave hits the WEC. Hence, motions coming from different directions will cause tension and compression forces on the dampers.

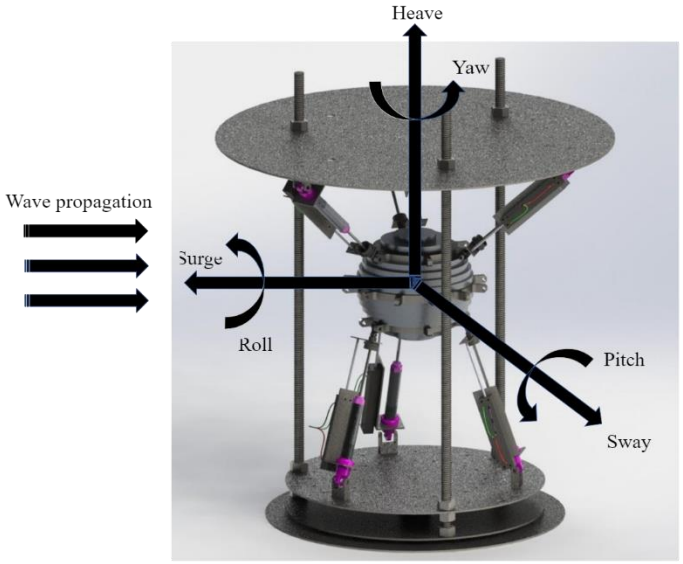

Fig. 2 TALOS II PTO system with six-degrees of freedom.

TALOS numerical modelling is based on a full-sized physical model of the device (Sheng et al., 2022a). The incoming wave is generated with an average 10s time period. In the measurements, a total of 20 variables are monitored, which are water surface elevation, surge motion, heave motion, pitch motion, PTO force in the x direction, PTO force in the z direction, PTO moment in the y direction, forces applied on six PTOs, electric power generated by six PTOs, and total power, respectively.

LSTM

The LSTM network consists of stacks of LSTM nets. The basic structure of the LSTM network is shown in Fig.2 (Liu et al., 2019). One LSTM net includes input gates, forget gates, cell state, output gates, sigmoid gates, and tanh gates. Unlike other machine learning algorithms, the LSTM emphasises on the importance of relationship between previous state and current state. The output of current state is determined by the current input X_t and the previous outputs the $h_{t-1,}$ and h_{t-2}. Note that the $h_{t-1,}$ and h_{t-2} are the output from previous states. The previous cell state (C_{t-1}) and the previous hidden state (h_t) are preserved and passed to the current cell state (C_t) and the current hidden state (h_t) without any losses. The sigmoid function (σ) which connects to previous states and current states is used to decide which input data need to be added or removed from cell state. Thus, the long-term dependency problem can be avoided.

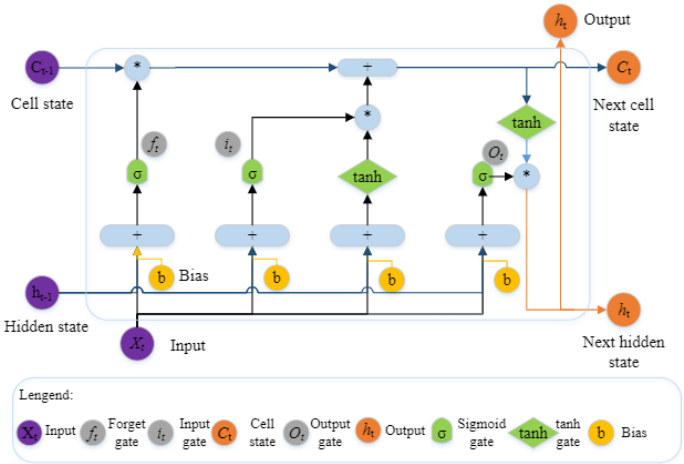

Fig.2 LSTM structure.

To determine whether to keep or remove the input (X_t) at time t, the decision function of forget gate (f_t) is considered. The decision function is ranged from 0 to 1 corresponding to the numbers in the cell state C_{t-1}, where the W_f and b_f are the weight and bias of forget gate, respectively.

$$f_t = \sigma（W_f[h_{t-1}, X_t] + b_f) \quad (1)$$

Then the sigmoid function is employed to decide whether the new information needs to be preserved or forgotten. Different with sigmoid function, the *tanh* function is used to determine the importance of the information to be transmitted from previous state. By multiplying the results from sigmoid function and *tanh* function, the new current state C_t is constructed from C_{t-1}.

$$i_t = \sigma(W_i[h_{t-1}, X_t] + b_i) \quad (2)$$
$$C_t = C_{t-1}f_t + tanh(W_n[h_{t-1}, X_t] + b_n)i_t \quad (3)$$

The current input gate i_t is constructed from a sigmoid function, which is calculated from previous hidden state and input, where the W_i and b_i are the weight and bias of the input gate. The current cell state C_t is determined by previous cell state C_{t-1}, forget gate f_t and *tanh* function.

The output of the LSTM is computed from the hidden state (h_t) at the current time t based on the output gate O_t.

$$O_t = \sigma（W_o[h_{t-1}, X_t] + b_o) \quad (4)$$
$$h_t = O_t tanh(C_t) \quad (5)$$

The output cell state is calculated from the sigmoid function of previous hidden state h_{t-1} and X_t, where the W_o and b_o are the weight and bias of the output gate, respectively. The output/ current hidden state is decided by the current output gate O_t and *tanh* function of current cell sate C_t.

The LSTM network is developed from RNN (Recurrent Neural Network). Thus, it has advantages in linking previous information to current state compared with other machine learning algorithms such as regression tress, SVR and ANN. Due to this characteristic, the LSTM is suitable for regression modelling for predicting and processing long-term time series data. This advantage has also been approved by many researchers (Jalayer et al., 2021; Abdul et al., 2020; and Zhao et al., 2016).

Power generation forecasting framework

To implement the proposed model, a five-step modelling method is used. The details of the power generation forecasting framework are shown in the Fig.3.

The raw data were acquired from the TALOS WEC numerical modelling in previous research with 0.05s sampling intervals, which included 20 monitoring variables (Sheng et al., 2022b). The first step is to pre-process the raw data including separate data into inputs and targets for the training dataset, inputs and targets for testing data, and data normalisation. Considering the causality of the WEC system, water surface elevation, surge motion, heave motion, pitch motion, PTO force in the x direction, PTO force in the z direction, and overall moment in the y direction are used as the training input. The PTO forces in x and z direction are extracted from the relative motion between the ball and the hull. The six PTOs' forces are used as the target and forecasting output of the model. Another method is using all the inputs to predict the total power output. The six PTOs are working independently but might affect each other. For instance, if one damper was broken and stuck in a compression position, it would leave more space for other dampers' movements. The extra electricity power produced by other dampers might compensate for the broken one. Hence, it is necessary to model the six PTOs' forces separately.

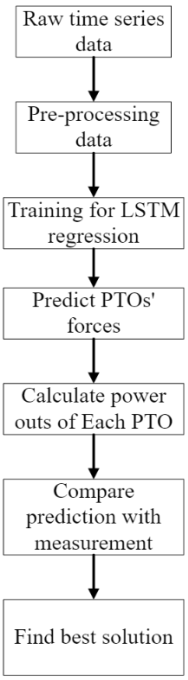

Fig. 3. TALOS WEC power generation model.

During the training process, the size of the dataset can affect training results significantly. Overtraining easily happens when the training set is too small. Larger datasets can help learning better but might consume massive computation resources. In this modelling, 12,0000 data were used with 90% data for training and 10% data for testing.

The second to fourth steps are setting training parameters for the LSTM model. The LSTM network parameter setting was based on previous success (Wu and Ma, 2022) and several tests by using the same dataset. The final hyperparameters were set with 250 max epochs, 1 gradient threshold, 0.05 initial learning rate, 125 drop period, and 0.2 drop factor After the training process is completed, the remaining 10% of the data is used for testing to validate the accuracy of the model. The forces of six PTOs are further used for the power outputs calculation by using Eq. 6.

$$P = \frac{F^2}{\lambda} \quad (6)$$

where P and F are the power output and force of one PTO and λ = 250,000 is the power coefficient based on hydrodynamic modelling.

Finally, the LSTM prediction accuracy is further compared with other machine learning algorithms. Both RMSE (root mean square error) in Eq. 7 and R^2 (coefficient of determination) in Eq. 8 are calculated to evaluate the forecasting model accuracy.

$$RMSE = \sqrt{\frac{\sum_{n=1}^{N}(\hat{y_n} - y_n)^2}{N}} \quad (7)$$

where $\hat{y_n}$ represents for the prediction value and y_n represents for the measurement value. The RMSE value is ranged from 0 to $+\infty$. Lower values indicate higher accuracy.

$$R^2 = 1 - \frac{SS_{res}}{SS_{tot}} \quad (8)$$

where SS_{res} and SS_{tot} represent for the residual sum of squares and total sum of squares, respectively. Normally, the R^2 value is ranged from 0-1. A value of 1 indicates the prediction model fits the data perfectly. If the value is calculated outside this range, that would indicate the prediction model does not fit the data at all.

POWER GENERATION RESULTS AND ANALYSIS

LSTM forecasting results

The TALOS WEC consists of six PTOs, labelled from 1st to 6th. Each PTO force is predicted based on the proposed LSTM regression method and the six PTO power output are further calculated. The predicted PTO forces, power outputs, and their corresponding R^2 values are demonstrated in Fig. 4-9.

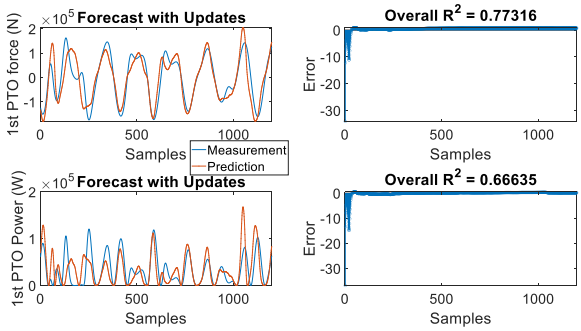

Fig.4 Forecasting results of first PTO force and power output.

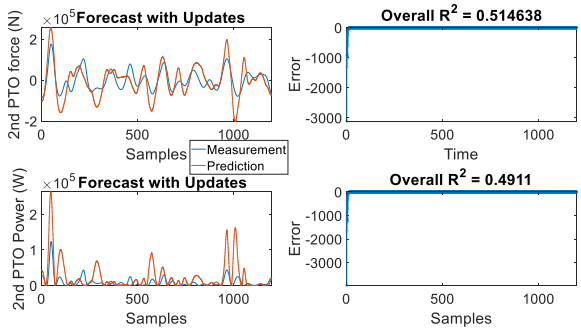

Fig. 5 Forecasting results of second PTO force and power output.

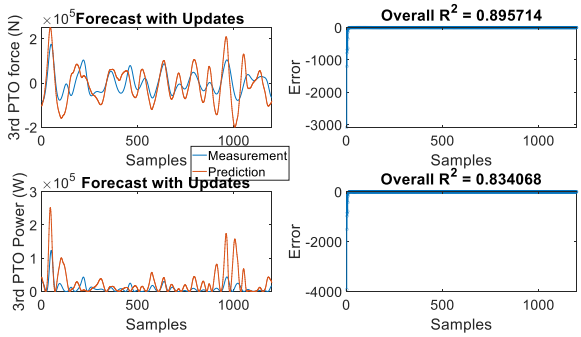

Fig. 6 Forecasting results of third PTO force and power output.

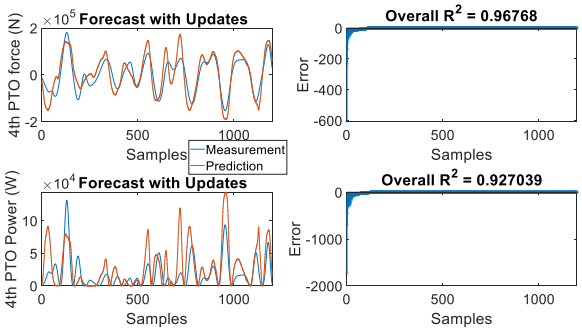

Fig. 7 Forecasting results of fourth PTO force and power output.

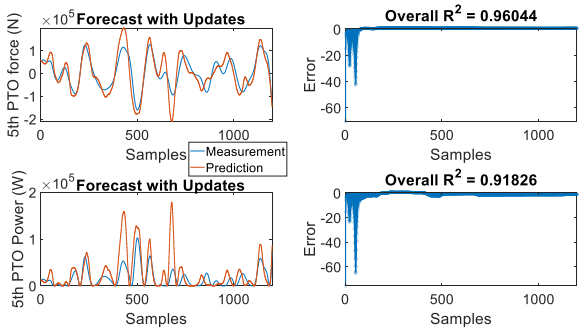

Fig. 8 Forecasting results of fifth PTO force and power output.

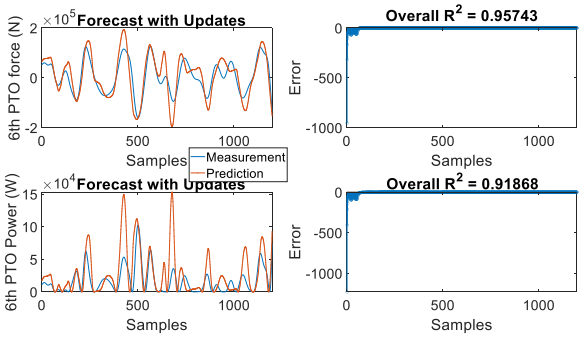

Fig. 9 Forecasting results of sixth PTO force and power output.

The six figures show the LSTM forecasting test results. Totally 1200 rows of data are used (10% of 12,000). In each case, the top-left subplot of the figures are the PTO forces predicted by the model. The top-right of the figures are the R^2 values calculated by the Eq.7. The bottom-left of the figures are the PTO power outputs produced from PTO forces. The bottom-right of the figures are the R^2 values based on power outputs calculation.

It can be observed from the figures that the overall performance of the prediction model is relatively high. However, when the measurement data change sharply, the model cannot capture the change instantly. Besides, the overall R^2 value graphs show how the R^2 value changes when the input data are increasing. The overall R^2 value is the average for all the testing data. It is also noticed that the power prediction accuracy is slightly lower than forces predictions. This is due to the non-linear calculation process that enlarges the prediction error.

Power output forecasting accuracy comparison

The LSTM is a type of deep learning algorithms. Hence, the complexity of its structure will cause heavier computation load and thus increase the processing time compared to other methods. Compared with LSTM, the regression tree, SVR and ANN have simpler structure and thus lead to faster processing speeds. Hence, it is necessary to compare the forecasting accuracy with other machine learning algorithms. In this paper, the overall R^2 values and RMSE values of the four mentioned algorithms are compared in Table.1.

Table 1. Prediction accuracy of four algorithms.

	LSTM	Regression tree	SVR	ANN
1st PTO R^2	0.67	0.44	0.78	0.56
2nd PTO R^2	0.49	0.56	0.67	0.45
3rd PTO R^2	0.83	0.75	0.74	0.78
4th PTO R^2	0.93	0.74	0.74	0.77
5th PTO R^2	0.92	0.52	0.81	0.83
6th PTO R^2	0.92	0.79	0.89	0.80
1st PTO RMSE	0.13	0.17	0.13	0.16
2nd PTO RMSE	0.15	0.16	0.14	0.17
3rd PTO RMSE	0.11	0.14	0.13	0.13
4th PTO RMSE	0.08	0.13	0.13	0.13
5th PTO RMSE	0.09	0.13	0.12	0.12
6th PTO RMSE	0.09	0.13	0.11	0.12

Table.1 shows the accuracy of four algorithms including both overall R^2 values and overall RMSE values of six PTOs' power output prediction. It can be observed from the table that some of the predictions produced by other algorithms have better accuracy. For example, in Table 1, in the case of the 2nd PTO, SVR makes the best prediction (smallest RMSE), while in the case of the 1st PTO, both SVR and LSTM have the same accuracy. However, the LSTM has the best performance in overall predictions. Among the four algorithms, the regression tree has the least complicated structure and the worst performance. Meanwhile, SVR and ANN have similar performance and are slightly worse than LSTM. In other words, the other three algorithms also prove the superior LSTM prediction ability.

CONCLUSIONS

This article has compared a novel LSTM approach with several other ML approaches for the prediction of power generation from a multi-DOF WEC presently in development. The work is presently limited to the analysis of simulated data. It is concluded from the results that LSTM offers a feasible approach for such power generation forecasting. On the basis of two types of tests and metrics, the LSTM algorithm yields improved performance compared to several other, more conventional machine learning algorithms. With the development of power prediction methods, better design of WEC control systems and power management becomes feasible, especially for offshore power management.

The current work on hyperparameter selection for LSTM networks is based on prior knowledge and commonly used parameters. In other words, it selects hyperparameters manually, which might cause extra errors in the prediction. The next steps will consider algorithm optimisation work related to hyperparameter selection for the training model. Also, investigations into other potential algorithms might be suitable for power prediction in this multi-DOF WEC context.

ACKNOWLEDGEMENTS

This work was supported by the EPSRC, Grant number EP/V040561/1, UK, for the project Novel High-Performance Wave Energy Converters with advanced control, reliability and survivability systems through machine-learning forecasting (NHP-WEC).

REFERENCES

Abdul, Z.K., Al-Talabani, A.K., & Ramadan, D.O. (2020). A hybrid temporal feature for gear fault diagnosis using the long short-term memory. *IEEE Sensors Journal*, 20(23), 14444-14452.

Aggidis, G.A., & Taylor, C.J. (2017). Overview of wave energy converter devices and the development of a new multi-axis laboratory prototype. In 20th IFAC Triennial World Congress, 9–14 July, Toulouse, France. Elsevier, *IFAC–PapersOnLine*, 50(1), 15651–15656.

AquaBuOy. (2016). *Finavera aquabuoy*. http://www.global-greenhousewarming.com/Finavera-aquabuoy.html

AWS Ocean. (2016). Archimedes Waveswing submerged wave power buoy. http://awsocean.com/technology/archimedeswaveswing-submerged-wave-power-buoy

Bento, P.M.R., Pombo, J.A.N., Mendes, R.P.G., Calado, M.R.A., & Mariano, S.J.P.S. (2021). Ocean wave energy forecasting using optimised deep learning neural networks. *Ocean Engineering*, 219, 108372.

Bhatt, J., Carthy, J., Clark, T., Galea, S., Sutch, A., Tutt, A., & Walker, J. (2016). Optimisation and development of a multi-axis wave energy converter device (Master of Engineering Project Report). Engineering Department, Lancaster University.

Boyle, G., & Duckers, L. (2012). Renewable energy: Power for a sustainable future. OUP Oxford.

Darwish, A., & Aggidis, G.A. (2022). A review on power electronic topologies and control for wave energy converters. *Energies*, 15(23), 9174.

Desouky, M.A., & Abdelkhalik, O. (2019). Wave prediction using wave rider position measurements and NARX network in wave energy conversion. *Applied Ocean Research*, 82, 10-21.

Jalayer, M., Orsenigo, C., & Vercellis, C. (2021). Fault detection and diagnosis for rotating machinery: A model based on convolutional LSTM, Fast Fourier and continuous wavelet transforms. *Computers in Industry*, 125, 103378.

Li, G., Weiss, G., Mueller, M., Townley, S., & Belmont, M.R. (2012). Wave energy converter control by wave prediction and dynamic programming. *Renewable Energy*, 48, 392-403.

Liu, Y., Guan, L., Hou, C., Han, H., Liu, Z., Sun, Y., & Zheng, M. (2019). Wind power short-term prediction based on LSTM and discrete wavelet transform. *Applied Sciences*, 9(6), 1108.

Liu, Z., Wang, Y., & Hua, X. (2020). Prediction and optimization of oscillating wave surge converter using machine learning techniques. *Energy Conversion and Management*, 210, 112677.

McCabe, A.P., Bradshaw, A., Meadowcroft, J.A., & Aggidis, G. (2006). Developments in the design of the PS Frog Mk 5 wave energy converter. *Renewable Energy*, 31, 141–151.

Mousavi, S. M., Ghasemi, M., Dehghan Manshadi, M., & Mosavi, A. (2021). Deep Learning for Wave Energy Converter Modeling Using Long Short-Term Memory. *Mathematics*, 9(8), 871.

Ni, C., Ma, X., & Bai, Y. (2018, September). Convolutional Neural Network based power generation prediction of wave energy converter. *In 2018 24th International Conference on Automation and Computing (ICAC)* (pp. 1-6). IEEE.

Orecon. (2009). Renewable Energy Focus, Wave energy developer Orecon hits stormy waters. http://www.renewableenergyfocus.com/view/5700/wave-energy-developer-orecon-hits-stormy-waters

Peña-Sánchez, Y., García-Abril, M., Paparella, F., & Ringwood, J. V.

(2018). Estimation and forecasting of excitation force for arrays of wave energy devices. *IEEE Transactions on Sustainable Energy*, 9(4), 1672-1680.

Powerbuoy. (2016). Ocean Power Technologies. http://www.oceanpowertechnologies.com/powerbuoytechnology

Reikard, G., Robertson, B., & Bidlot, J. R. (2015). Combining wave energy with wind and solar: Short-term forecasting. *Renewable Energy*, 81, 442-456. https://doi.org/10.1016/j.renene.2015.03.016

Salter, S. H. (1974). Wave Power. *Nature*, 249, 720–724.

Sheng, W., Tapoglou, E., Ma, X., Taylor, C. J., Dorrell, R. M., Parsons, D. R., & Aggidis, G. (2022a). Hydrodynamic studies of floating structures: Comparison of wave-structure interaction modelling. *Ocean Engineering*, 249, 110878.

Sheng, W., Tapoglou, E., Ma, X., Taylor, C. J., Dorrell, R., Parsons, D. R., & Aggidis, G. (2022b). Time-Domain Implementation and Analyses of Multi-Motion Modes of Floating Structures. *Journal of Marine Science and Engineering*, 10(5), 662.

Taylor, C. J., Bradshaw, A., Chaplin, R. V., French, M., & Widden, M. B. (2002). Wave Energy Research at Lancaster University: PS FRog and Frond. *World Renewable Energy Congress VII*, Cologne, Germany.

Wave power firm Pelamis calls in administrators. (2014, November 21). *BBC News*. http://www.bbc.co.uk/news/uk-scotland-scotland-business-30151276

Wave Hub. (2016). Carnegie Wave Energy Limited. http://www.wavehub.co.uk/wave-hub-site/ourcustomers/carnegie-wave-energy-limited

Wang, Y. (2020). Predicting absorbed power of a wave energy converter in a nonlinear mixed sea. *Renewable Energy*, 153, 362-374.

Wu, Y., & Ma, X. (2022). A hybrid LSTM-KLD approach to condition monitoring of operational wind turbines. *Renewable Energy*, 181, 554-566.

Zhang, J., Zhao, X., Jin, S., & Greaves, D. (2022). Phase-resolved real-time ocean wave prediction with quantified uncertainty based on variational Bayesian machine learning. *Applied Energy*, 324, 119711.

Zhao, R., Wang, J., Yan, R., & Mao, K. (2016, November). Machine health monitoring with LSTM networks. *In 2016 10th International Conference on Sensing Technology (ICST)* (pp. 1-6). IEEE.

Zou, S., Zhou, X., Khan, I., Weaver, W. W., & Rahman, S. (2022). Optimization of the electricity generation of a wave energy converter using deep reinforcement learning. *Ocean Engineering*, 244, 110363.